

Evidences for a dual population of CBC from sGRBs observations



Karelle Siellez

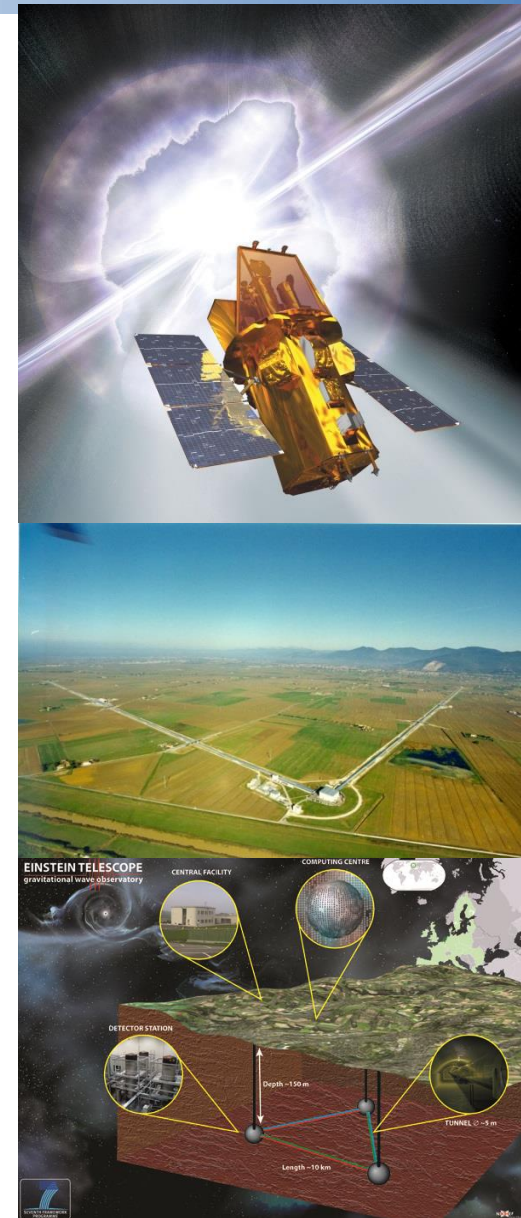
Michel Boér, Bruce Gendre & Tania Regimbau

ARTEMIS - Nice, France

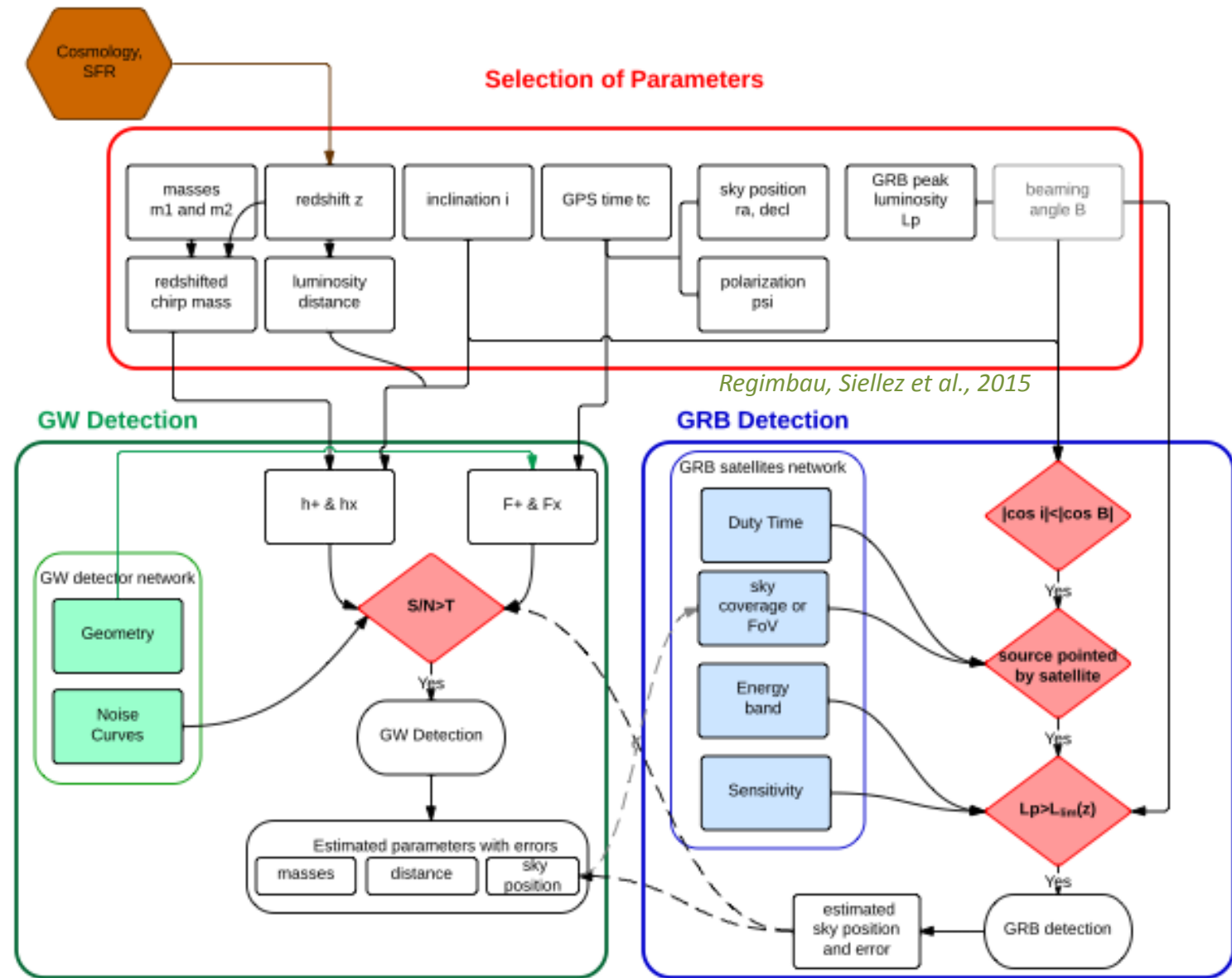
SF2A 2015, Toulouse, CA – 15/03/16

The link with GW

- **Link between gravitational waves and short GRBs**
 - They have possibly the same progenitor : the coalescence of compact objects
 - Rate estimation of simultaneous detection by gravitational wave and gamma ray needed
- **Why getting a coincident detection ?**
 - Improving the confidence of a GW detection by ALV
 - Improving knowledge about CBC progenitors
 - Targeted search with sGRB as a trigger to detect fainter signal with ALV
 - GW alert could increase the chance of an early detection
 - Obtaining a direct value of the cosmological constant



Process



Monte Carlo Simulations

Simulated sources with the following input parameters:

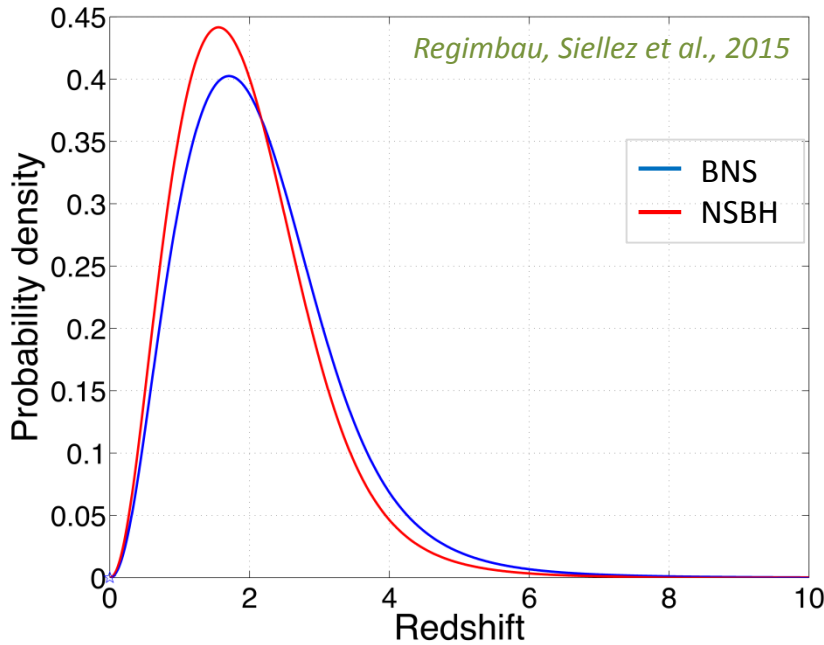
- **Polarisation, sky position, inclination:** Uniform distribution
- **Masses of each objects** with a delta function.
For NS : $m = 1.4 M_{\odot}$ and for BH: $m = 10 M_{\odot}$
- **Beaming angle** $\Theta_B = [5^\circ - 30^\circ]$
- **Intrinsic peak luminosity** L_p : broken power law with parameters derived from population synthesis (Guetta et al. 2005, Hopman et al. 06, Wanderman et al. 14):

$$\phi(L_p) \propto \begin{cases} (L_p / L_*)^{\alpha} & \text{if } L_* / \Delta_1 < L_p < L_* \\ (L_p / L_*)^{\beta} & \text{if } L_* < L_p < \Delta_2 L_* \end{cases}$$

with $\alpha = -0.6, \beta = -2, L_* = 10^{51} \text{ erg}, \Delta_1 = 100, \Delta_2 = 10$

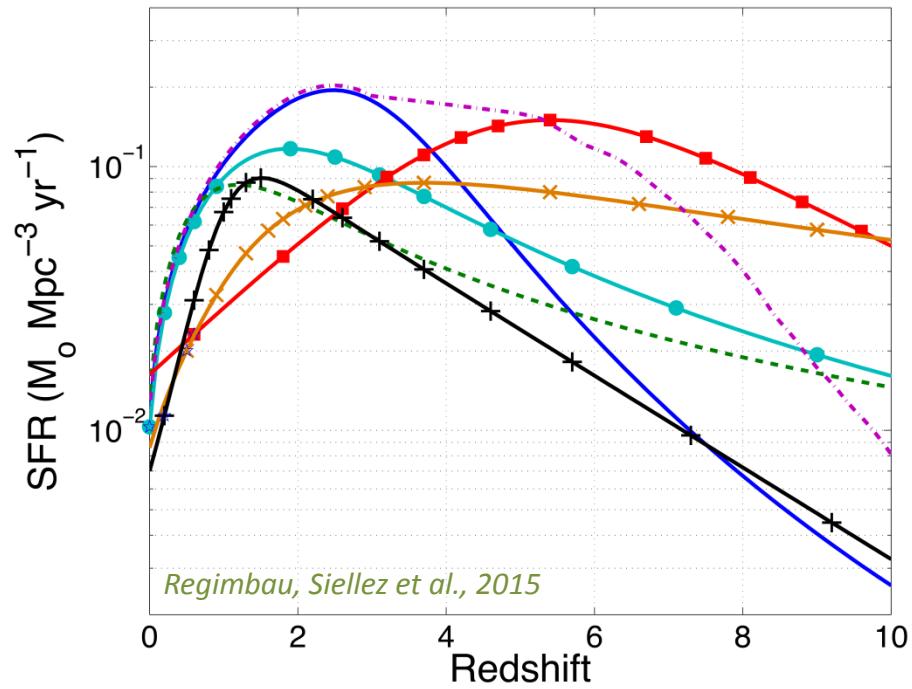
- **Rest Frame duration** : Gaussian distribution for $\log(T_i)$ derived from Zhang et al. 2012 with $\langle \log(T_i) \rangle = -0.46$ and $\sigma_{\log(T_i)} = 0.502$
- **Redshift:** Probability distribution of z

Redshift selection and SFR



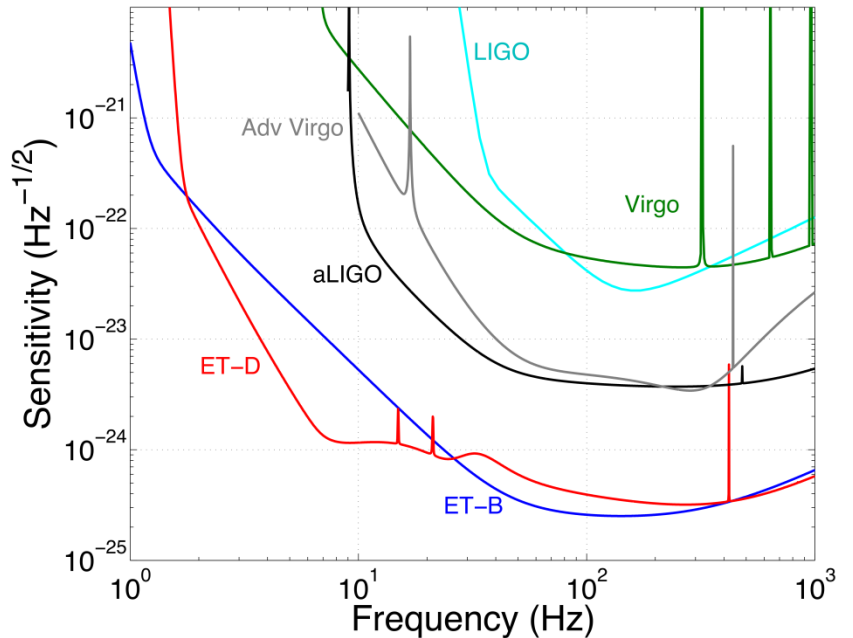
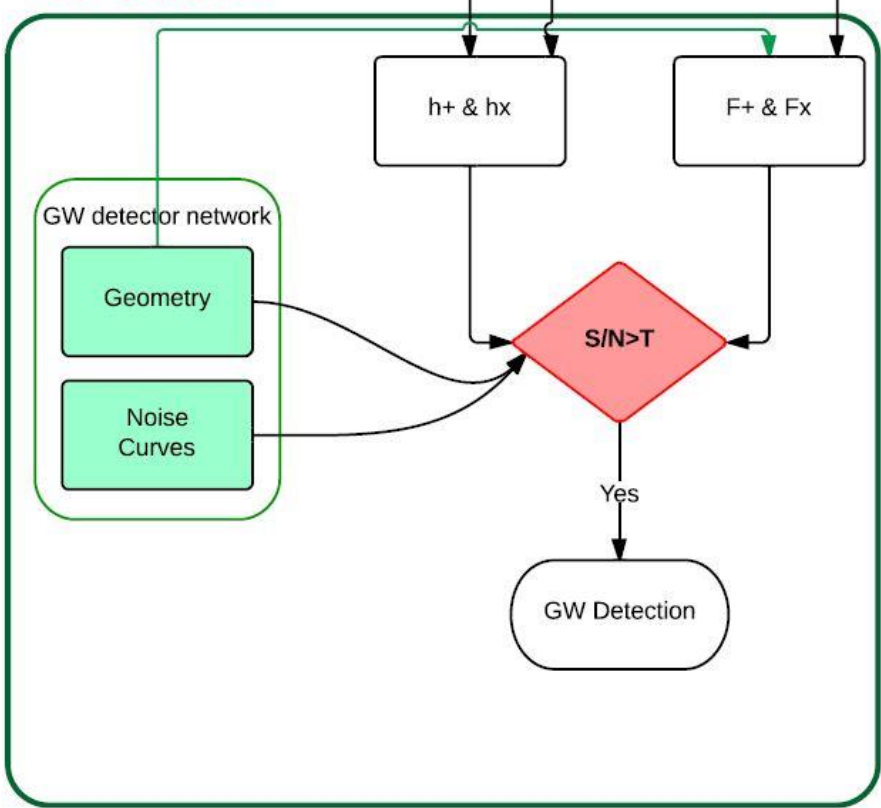
Different SFR:

Hopkins & Beacom 2006 (our reference model), Fardal et al. 2007, Wilkins et al. 2008, Springel & Hernquist 2003, Nagamine et al. 2006, Tornatore et al. 2007, Madau et al. 1998.



Gravitational wave detection

GW Detection



Regimbau et al., 2012, arXiv:1201.3563

SNR individual :

$$\rho_A^2 = \frac{5}{6} \frac{(GM_c(1+z))^{5/3} F_A^2}{c^3 \pi^{4/3} d_L^2(z)} \int_{f_{\min}}^{f_{LSO}} df \frac{f^{-7/3}}{S_{n,A}(f)}$$

with

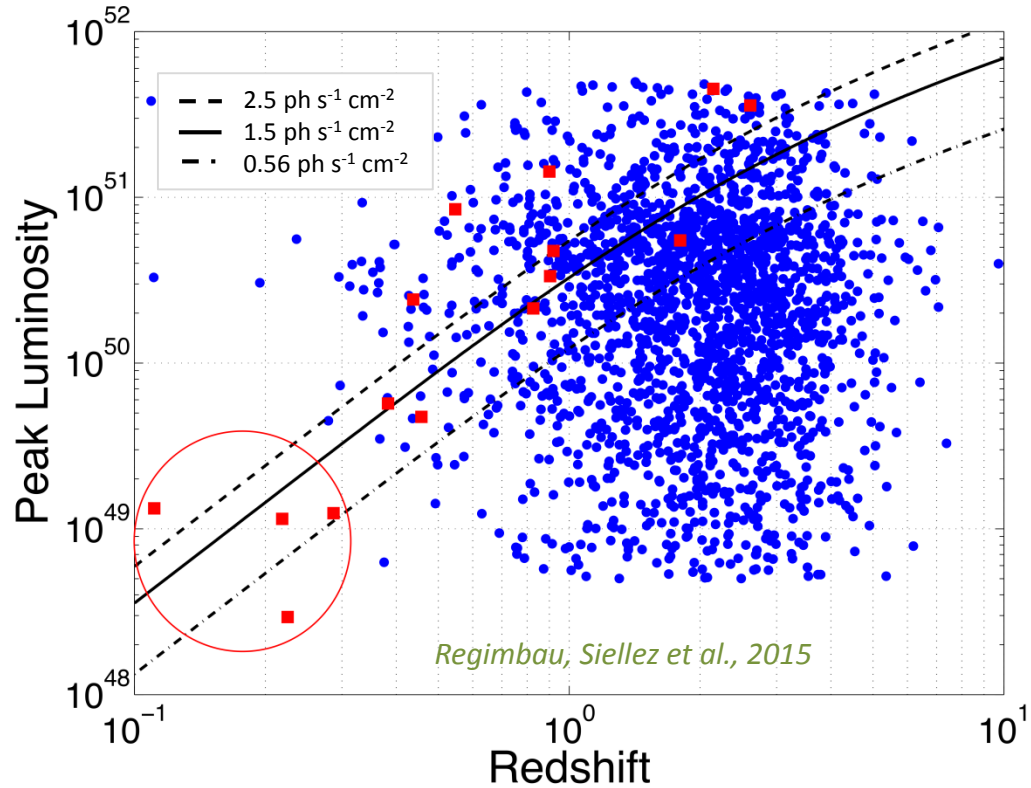
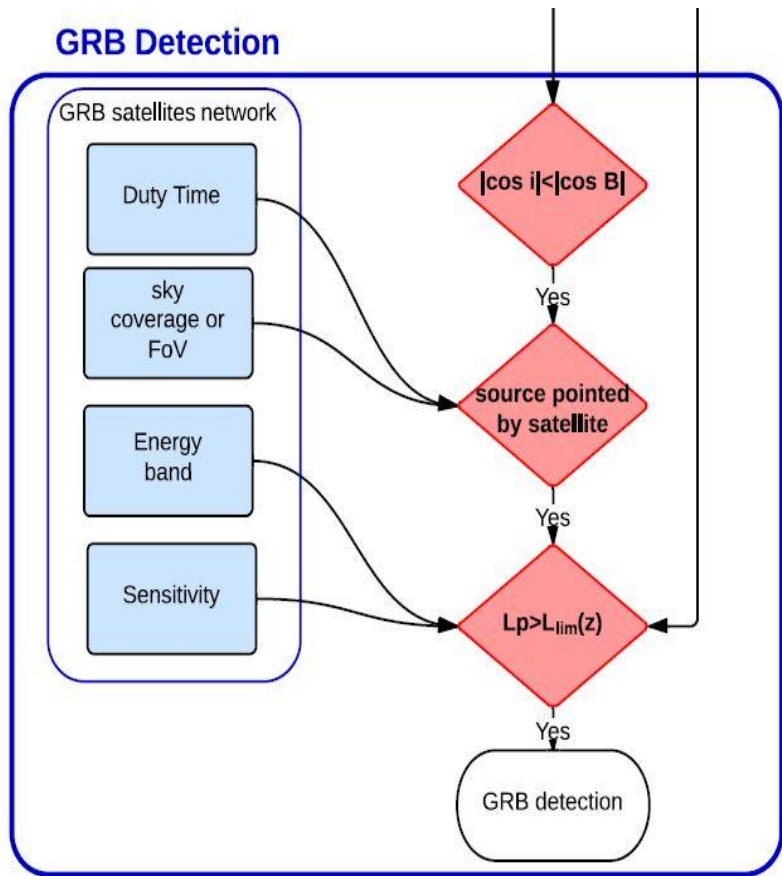
$$F_A^2 = \frac{(1+\cos^2 i)^2}{4} F_{+,A}^2(\Omega, \psi, t) + \cos^2 i F_{\times,A}^2(\Omega, \psi, t)$$

Coherent SNR:

$$\rho^2 = \sum \rho_A^2$$

Gamma-Ray Bursts detection

For *Swift*: $L_{\text{lim}}(z) = 4\pi d_L(z)k(z)F_{\text{lim}}$
Simulated sources and sGRBs observed
(Zhang, Z. B. et al. 2012, ArXiV: 1205.2411)



To observe 100% [80%, 50%] of the sources before $z \sim 1$:

$$F_{\text{lim}} = 0.025 \text{ ph s}^{-1} \text{ cm}^{-2} [0.26, 1.3]$$

Simultaneous simulated rate

ALV-Swift

	5°	10°	15°	20°	30°	GW
BNS						
$\rho_T = 12$	0.004 – 0.005	0.01 – 0.02	0.03 – 0.04	0.06 – 0.07	0.11 – 0.13	2.5 – 3.0
$\rho_T = 8$	0.01 – 0.02	0.05 – 0.07	0.10 – 0.13	0.17 – 0.23	0.35 – 0.46	
NS-BH						
$\rho_T = 12$	0.001 – 0.002	0.006 – 0.008	0.01 – 0.02	0.02 – 0.03	0.04 – 0.06	1.5 – 2.0
$\rho_T = 8$	0.004 – 0.007	0.02 – 0.03	0.04 – 0.05	0.06 – 0.10	0.12 – 0.19	

Regimbau, Siellez et al., 2015

ET – perfect detector

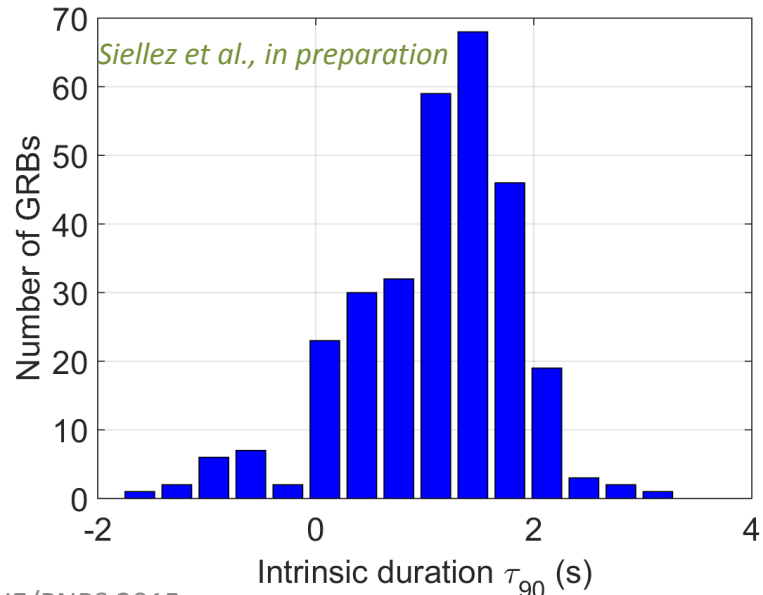
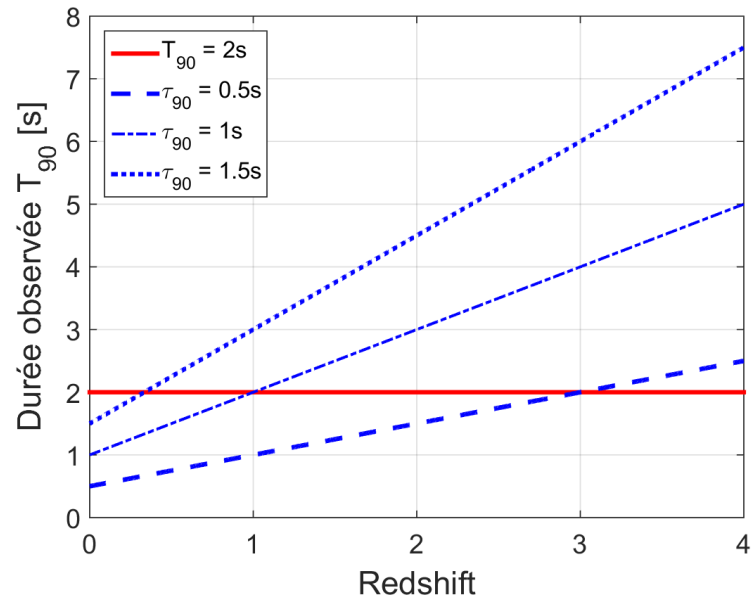
	5°	10°	15°	20°	30°	GW
BNS	$(0.8 - 1.8) \times 10^2$	$(3 - 7) \times 10^2$	$(0.7 - 1.6) \times 10^3$	$(1.3 - 2.8) \times 10^3$	$(2.5 - 5.8) \times 10^3$	$(0.6 - 1.5) \times 10^4$
NS-BH	7 – 15	27 – 61	59 – 136	104 – 239	228 – 517	$(1.3 - 2.4) \times 10^3$

Regimbau, Siellez et al., 2015

New sample of sGRBs

- Sample based on Swift observations
 - Redshift measurement

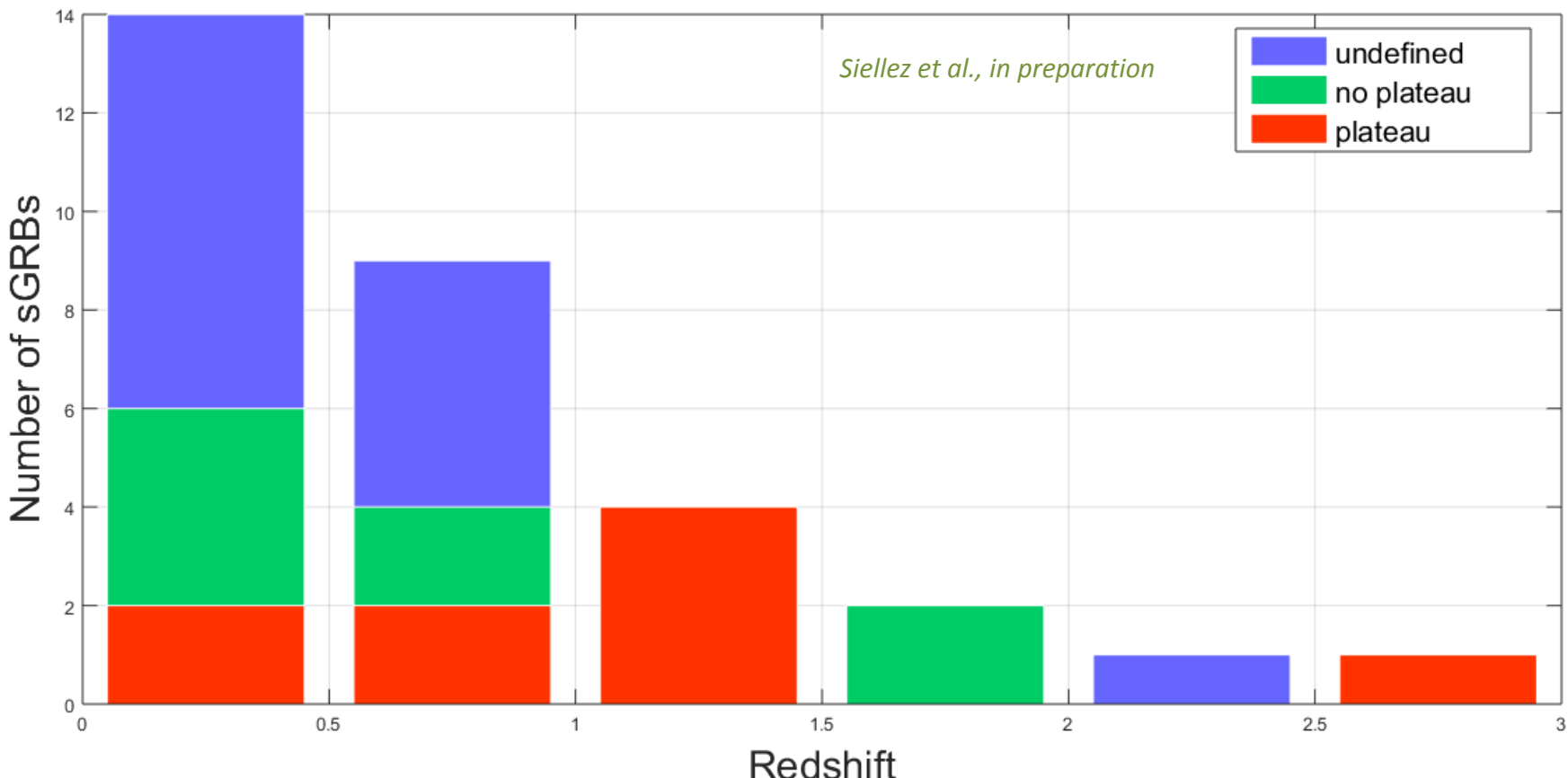
- Derivation of a sample of "true short" bursts
 - Use of the rest frame duration
 - Selection by hardness ratio
 - Bursts presenting a soft tail ?



New sample of sGRBs

Number of sGRBs : 31

- 14 unknown
- 8 no plateau phase
- 9 with plateau phase



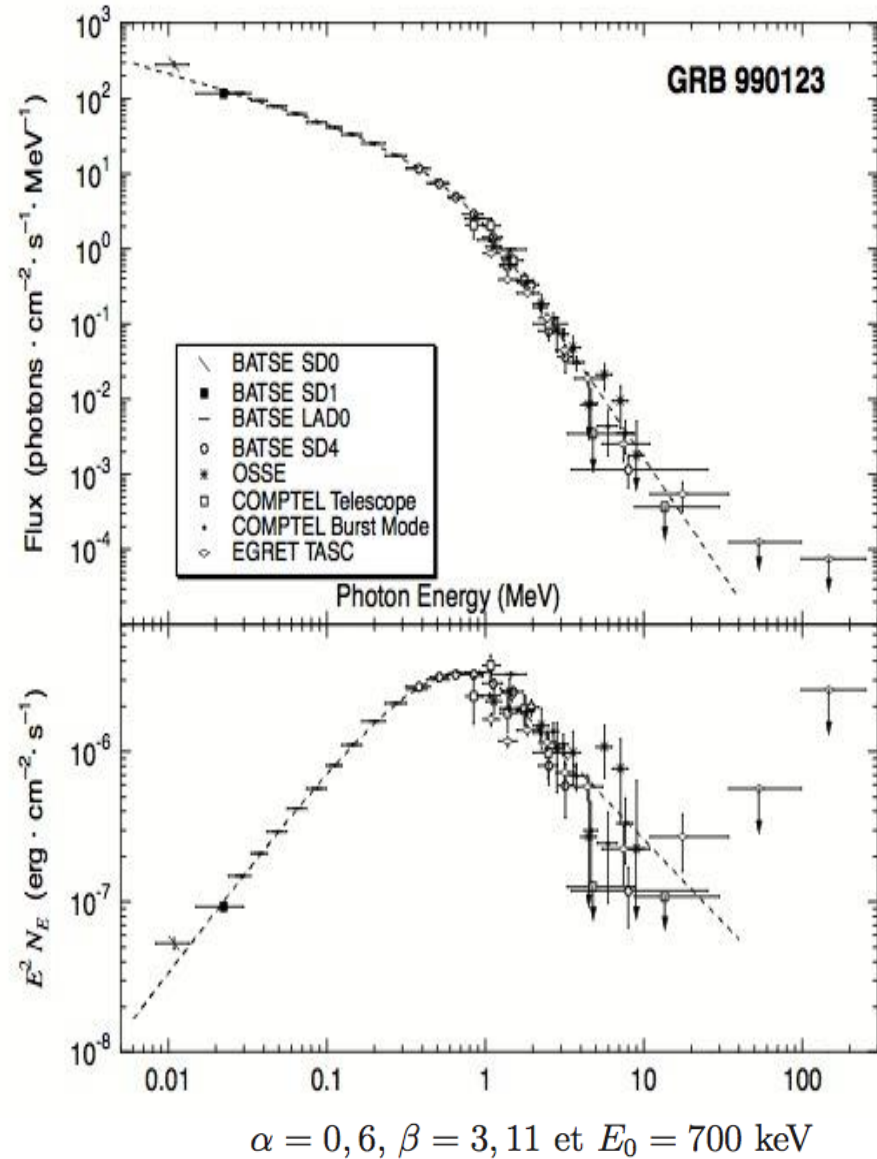
Data analysis

- **Instruments used**

- **KONUS (GCN)** : 8 sGRBs
- **HETE-2 (GCN)** : 1 sGRBs
- **GBM+BAT**: 7 sGRBs
 - 3 sGRBs : Virgili et al. 2012, MNRAS, 424, 2821.
 - 1 sGRBs : Sakamoto et al. 2013, ApJ, 766.
 - [+ 3 sGRBs : my own analysis incoming.]
- **BAT**: 18 sGRBs analysed

- **BAT Analysis**

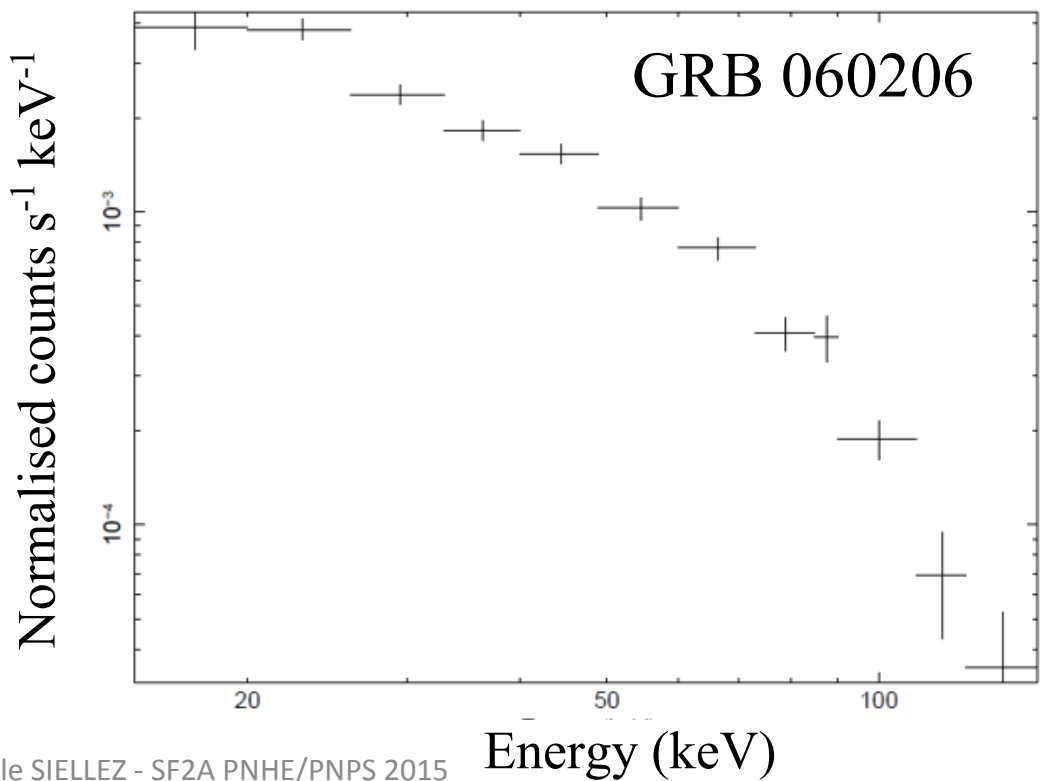
XSPEC + ftools



Data analysis

- **Instruments used**
 - **KONUS (GCN)** : 8 sGRBs
 - **HETE-2 (GCN)** : 1 sGRBs
 - **GBM+BAT**: 7 sGRBs
 - 3 sGRBs : Virgili et al. 2012, MNRAS, 424, 2821.
 - 1 sGRBs : Sakamoto et al. 2013, ApJ, 766.
 - [+ 3 sGRBs : my own analysis incoming.]
- **BAT**: 18 sGRBs analysed

- **BAT Analysis**
XSPEC + ftools

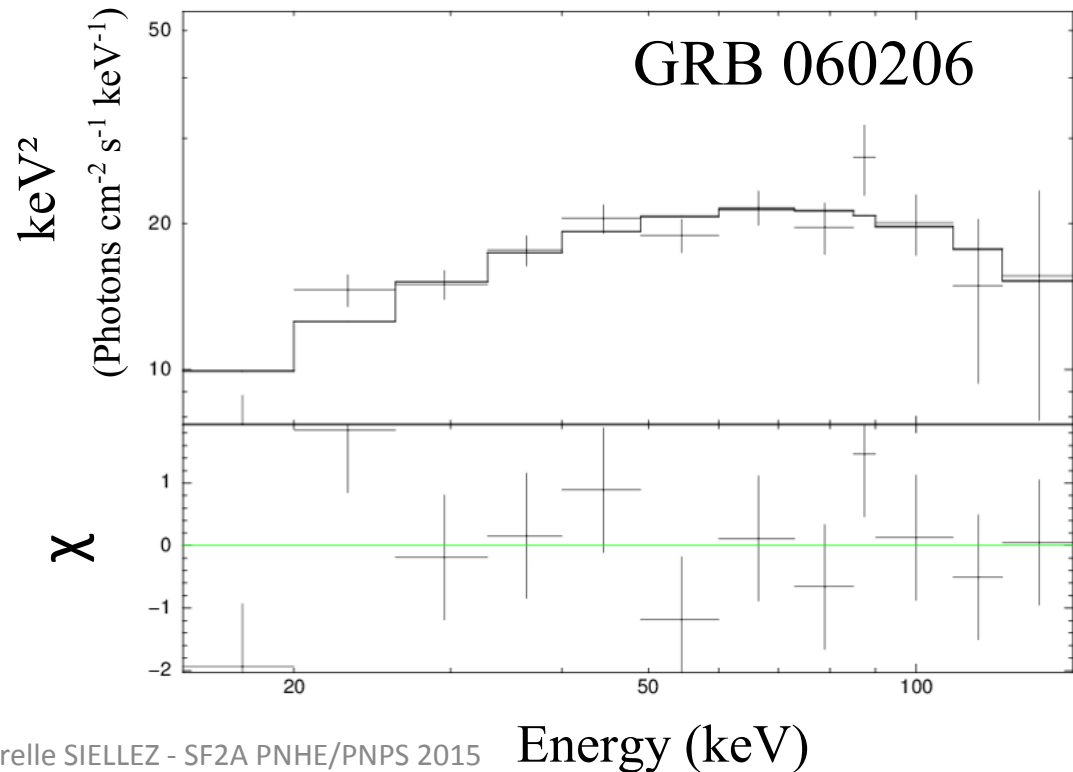


Data analysis

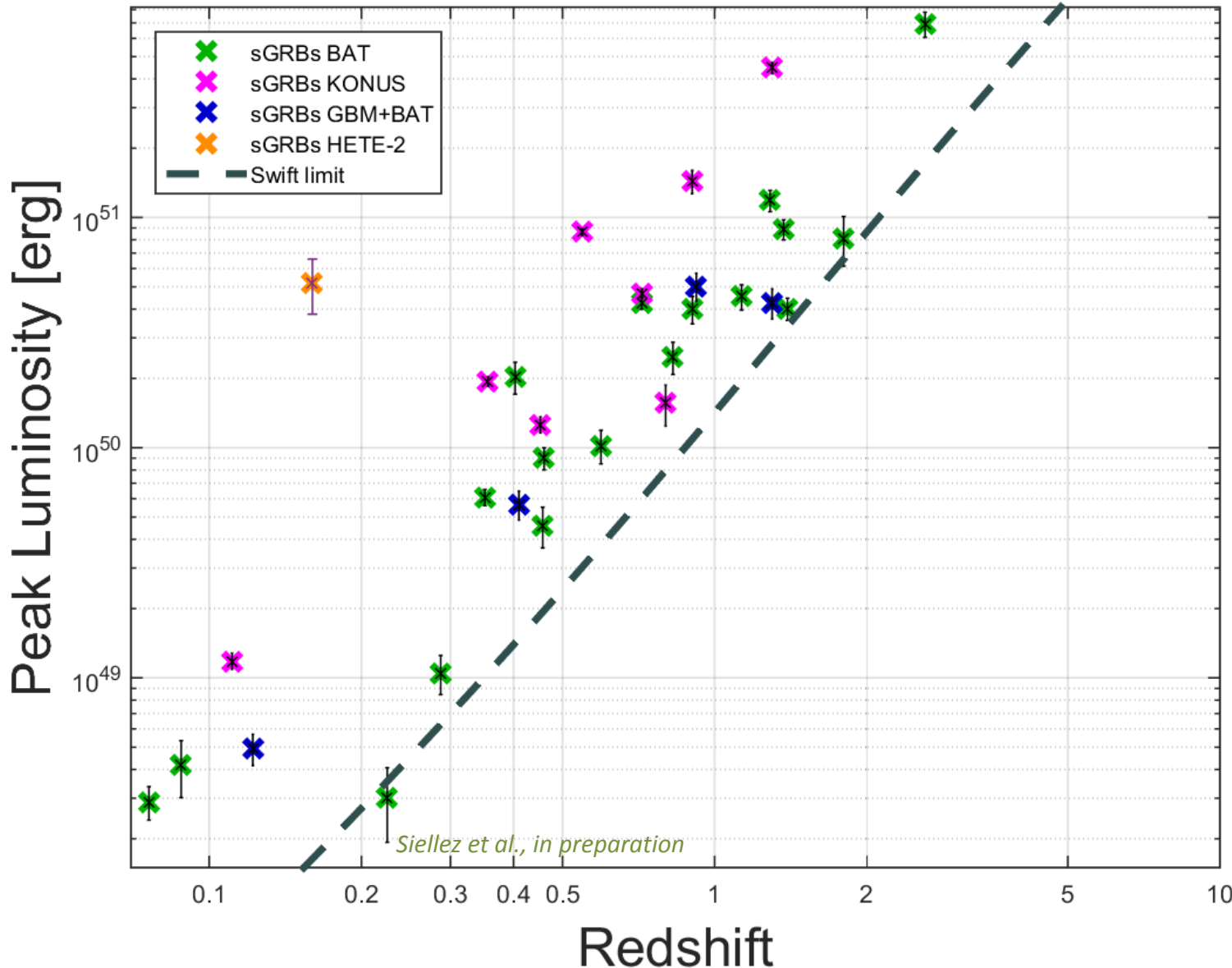
- **Instruments used**

- **KONUS (GCN)** : 8 sGRBs
- **HETE-2 (GCN)** : 1 sGRBs
- **GBM+BAT**: 7 sGRBs
 - 3 sGRBs : Virgili et al. 2012, MNRAS, 424, 2821.
 - 1 sGRBs : Sakamoto et al. 2013, ApJ, 766.
 - [+ 3 sGRBs : my own analysis incoming.]
- **BAT**: 18 sGRBs analysed

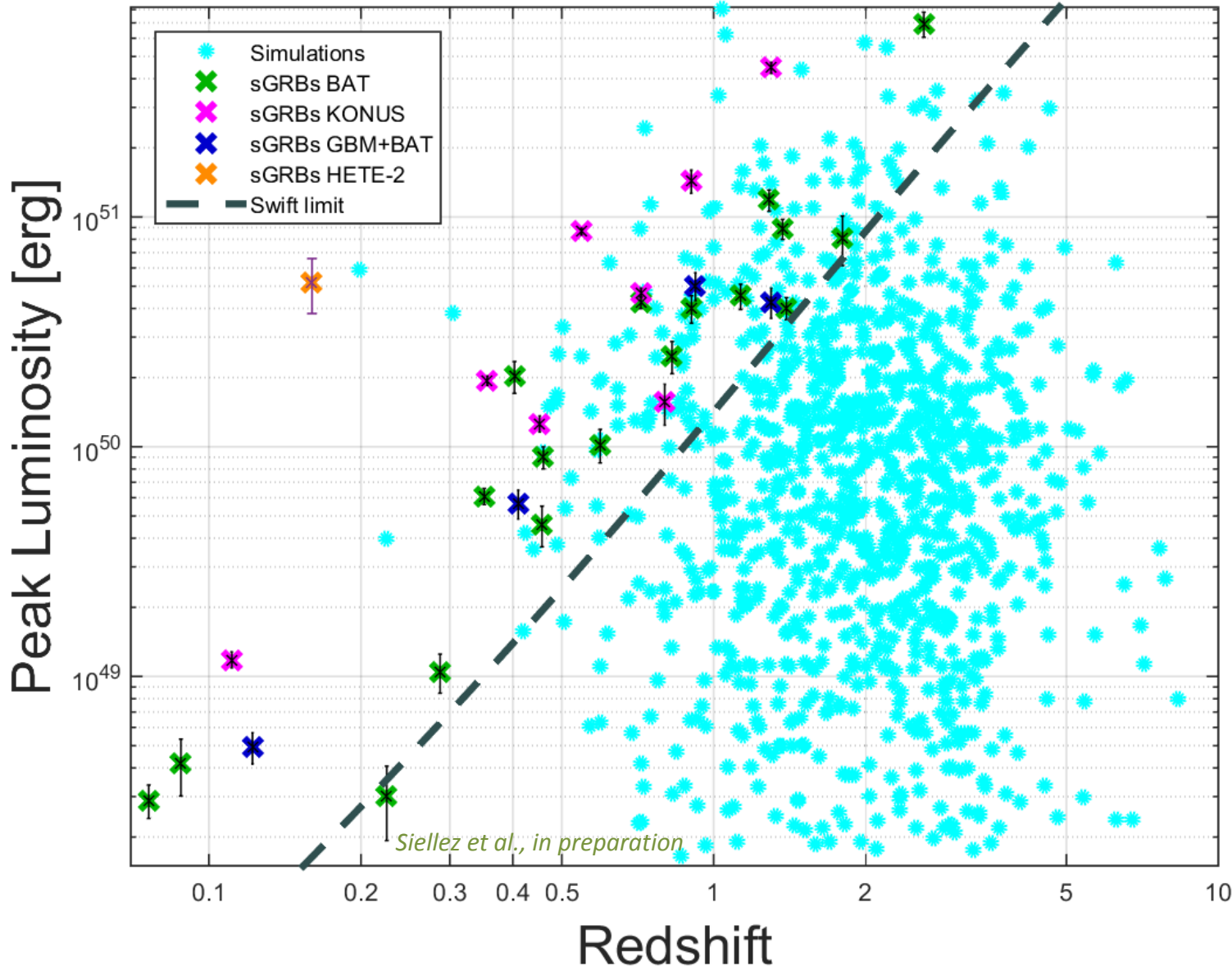
- **BAT Analysis**
Utilisation XSPEC.



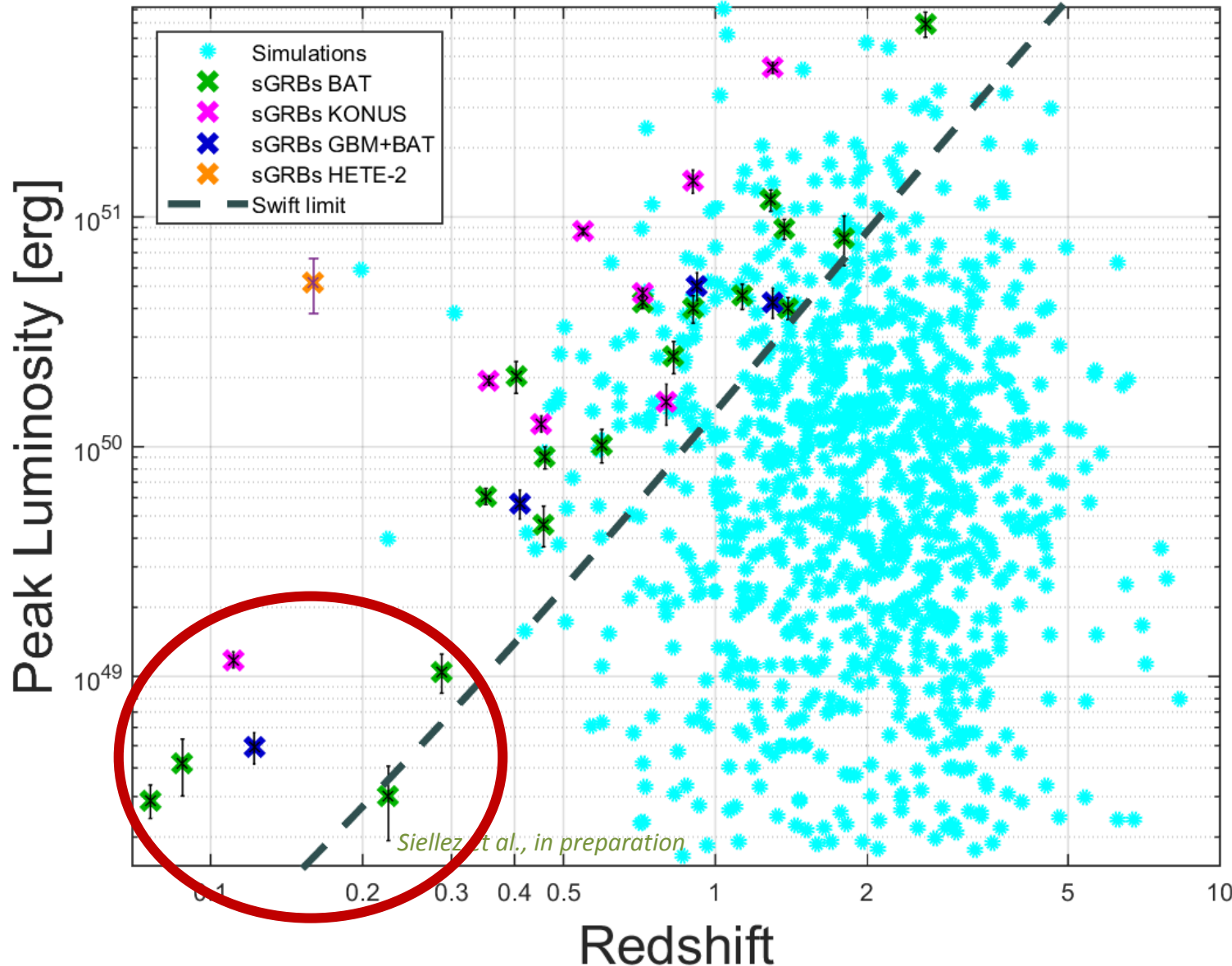
Lpeak (z) : different satellites



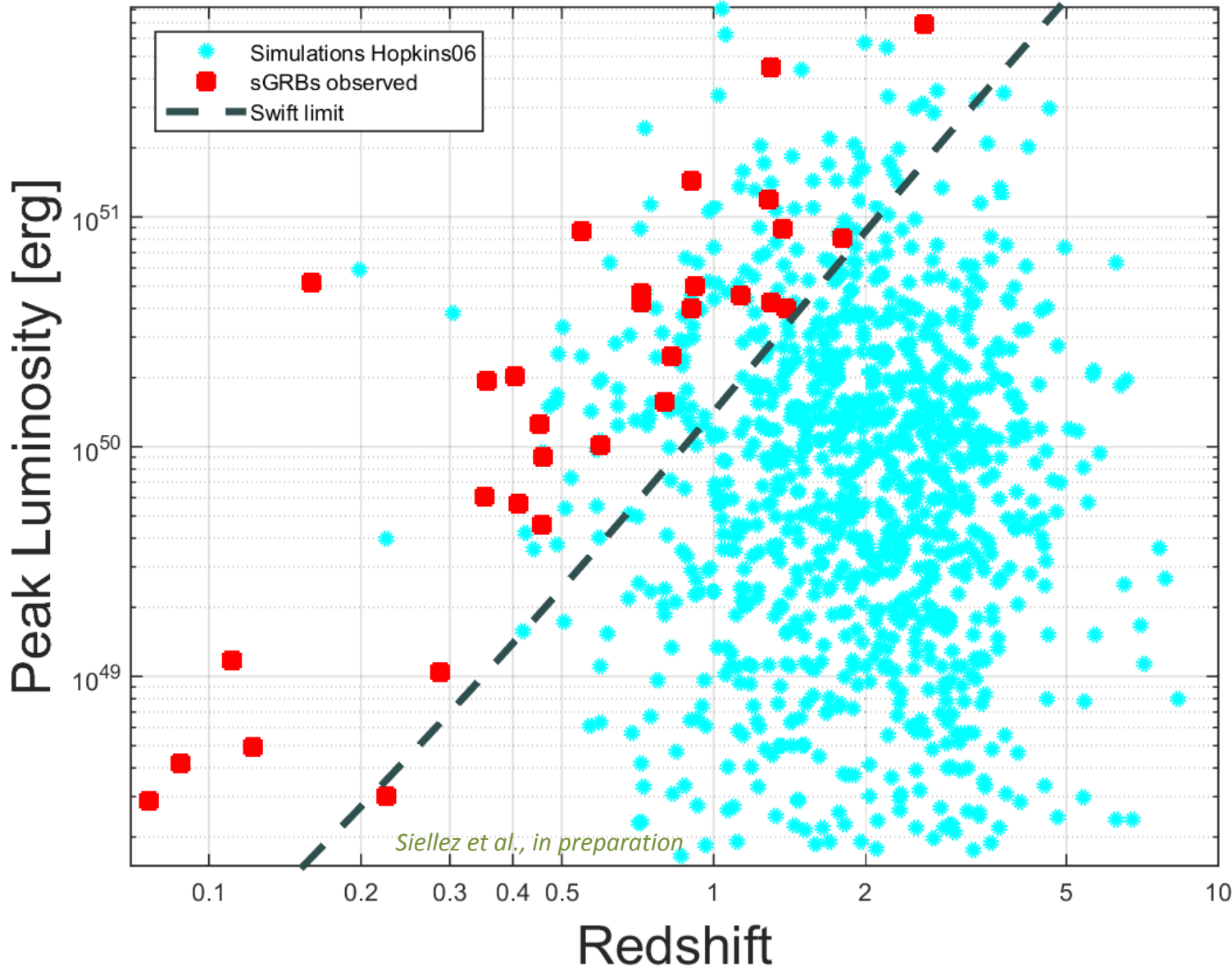
Lpeak (z) : Simulations Hopkins 06



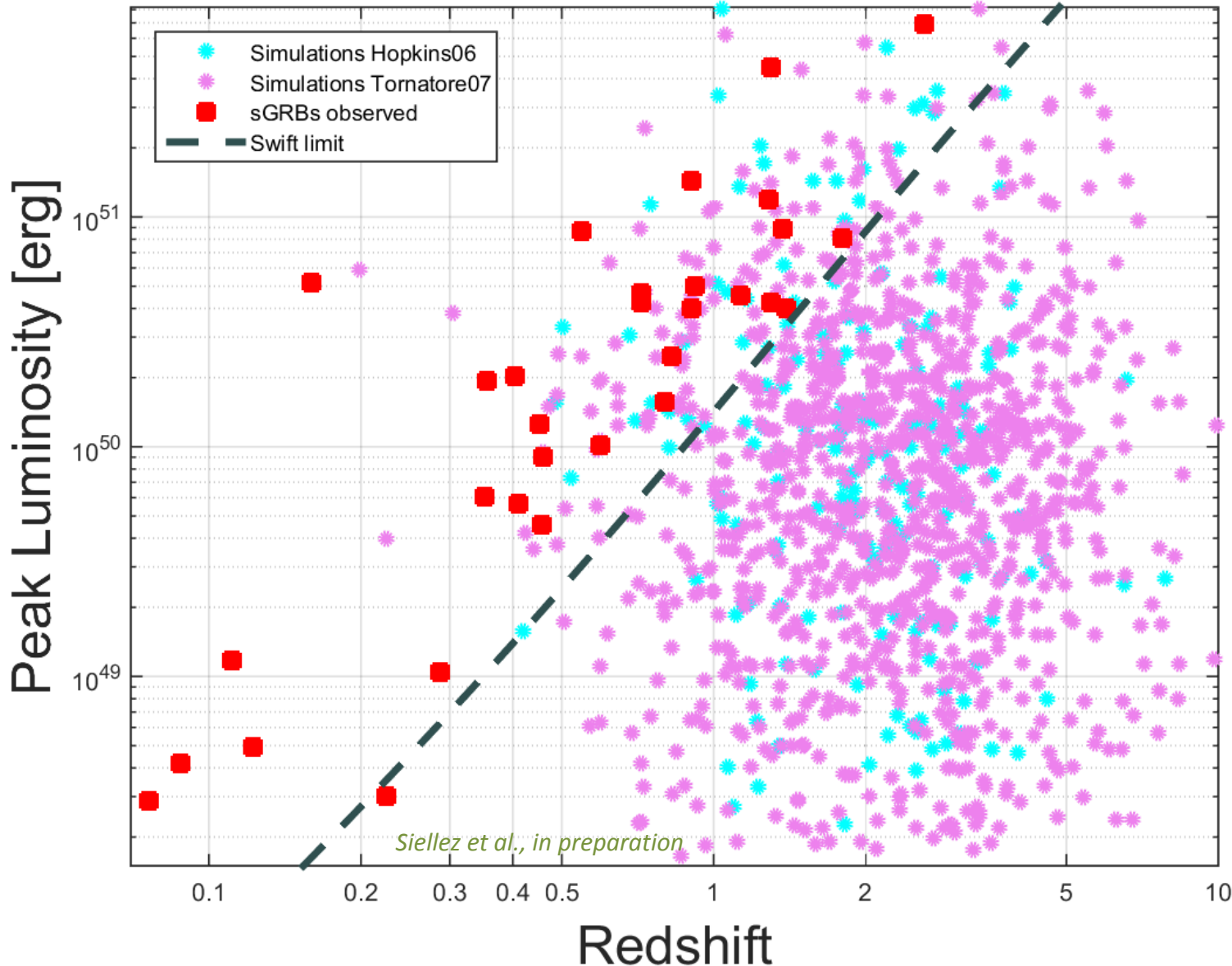
Lpeak (z) : Outlayers



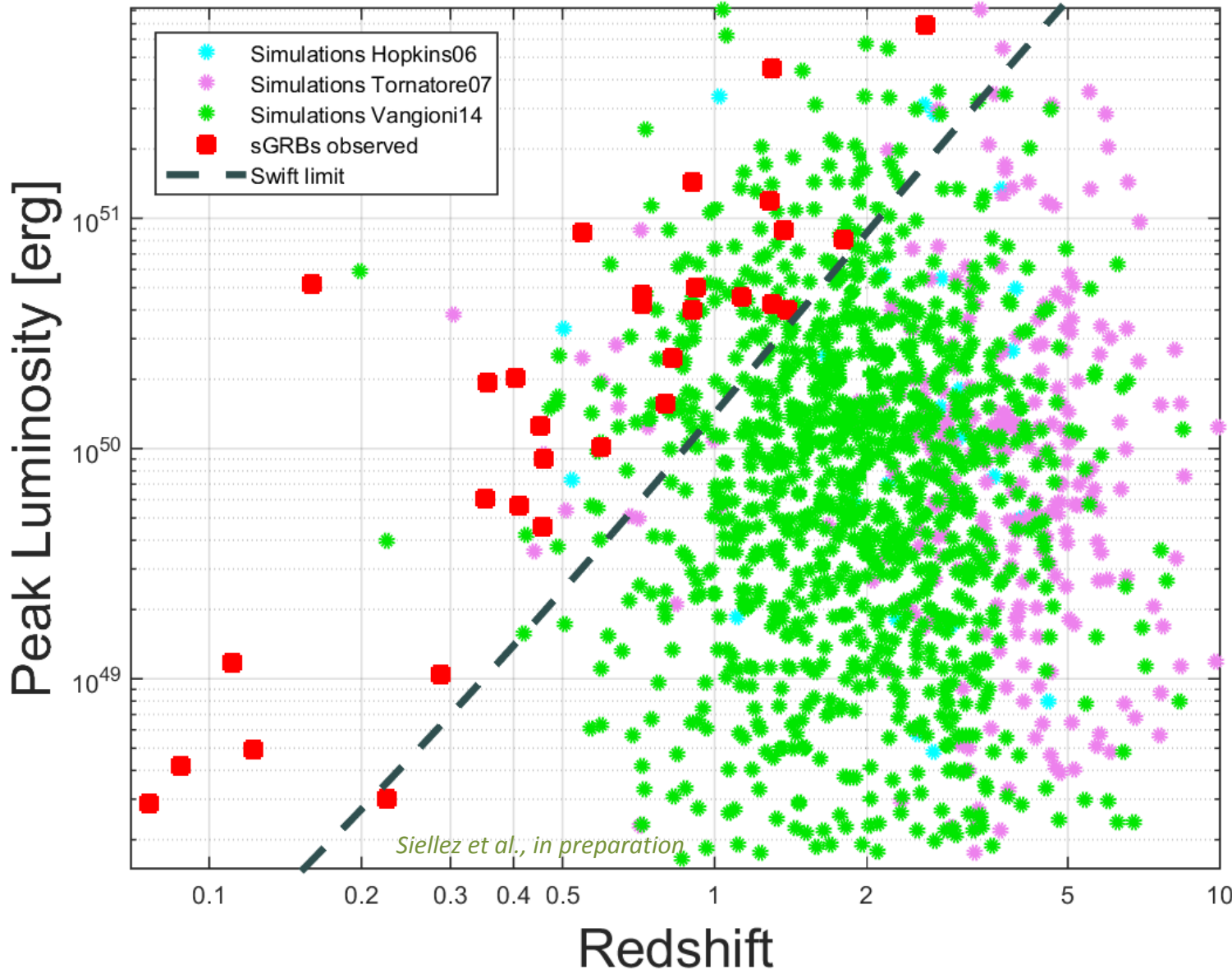
Lpeak (z) : Different SFR models



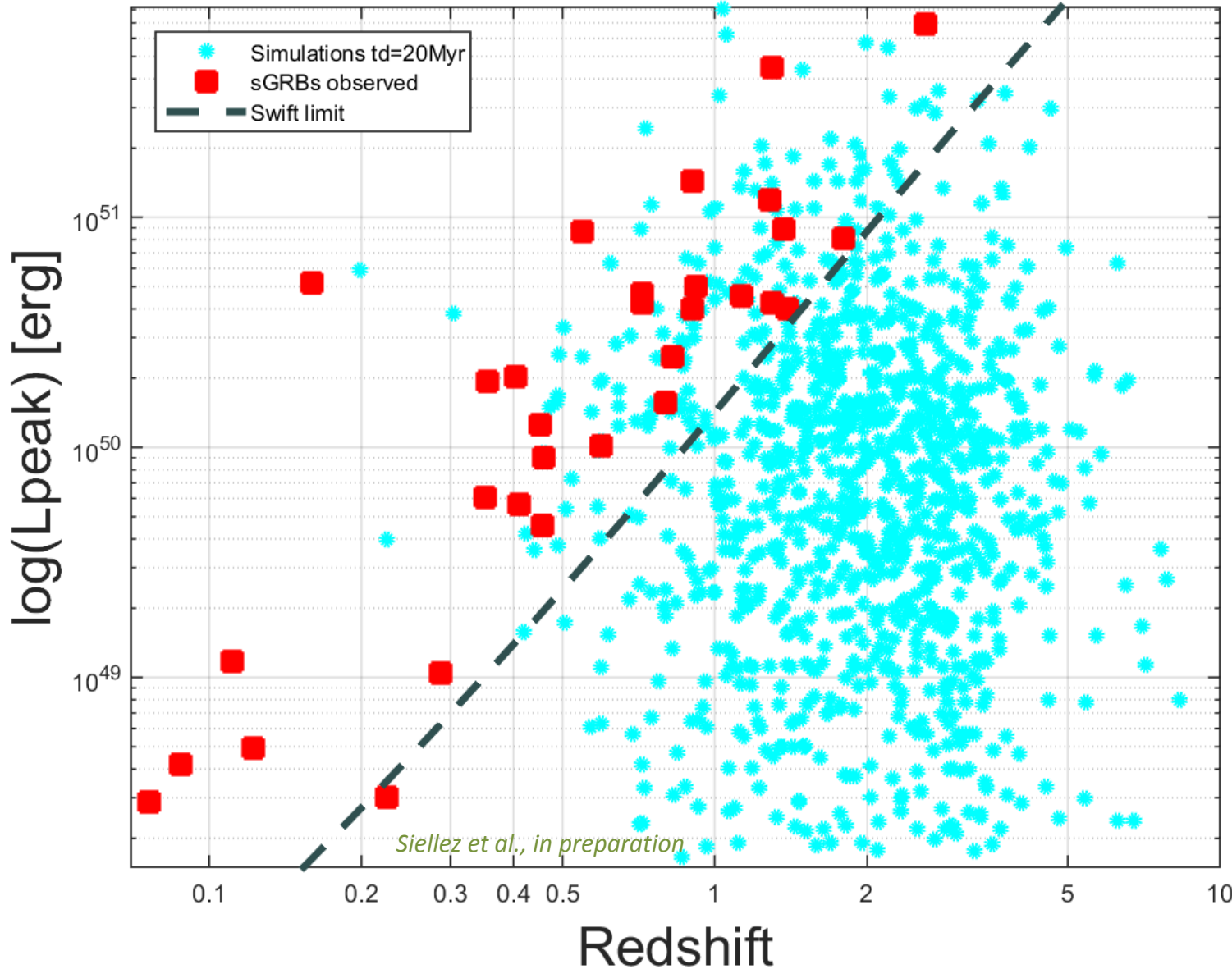
Lpeak (z) : Different SFR models



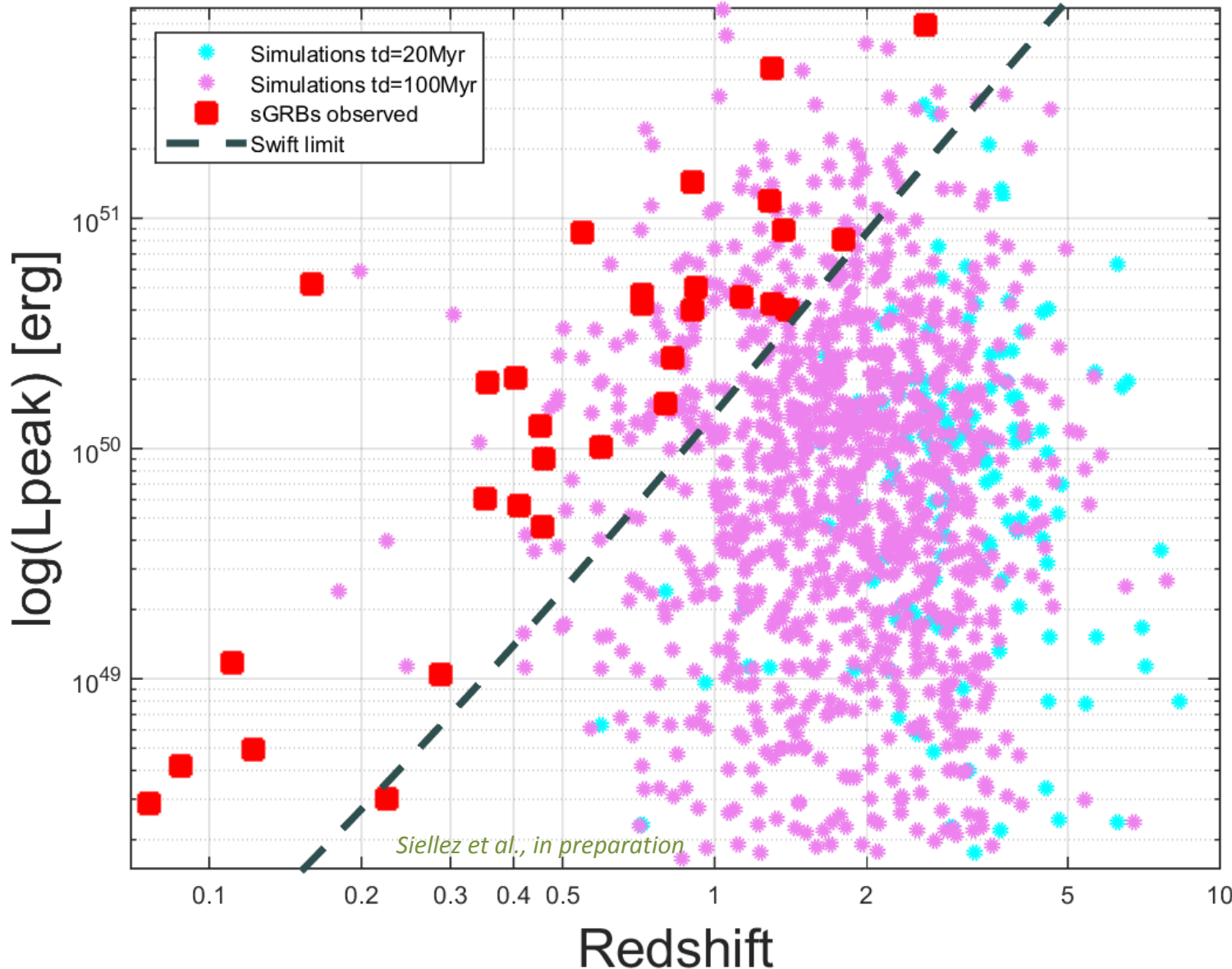
Lpeak (z) : Different SFR models



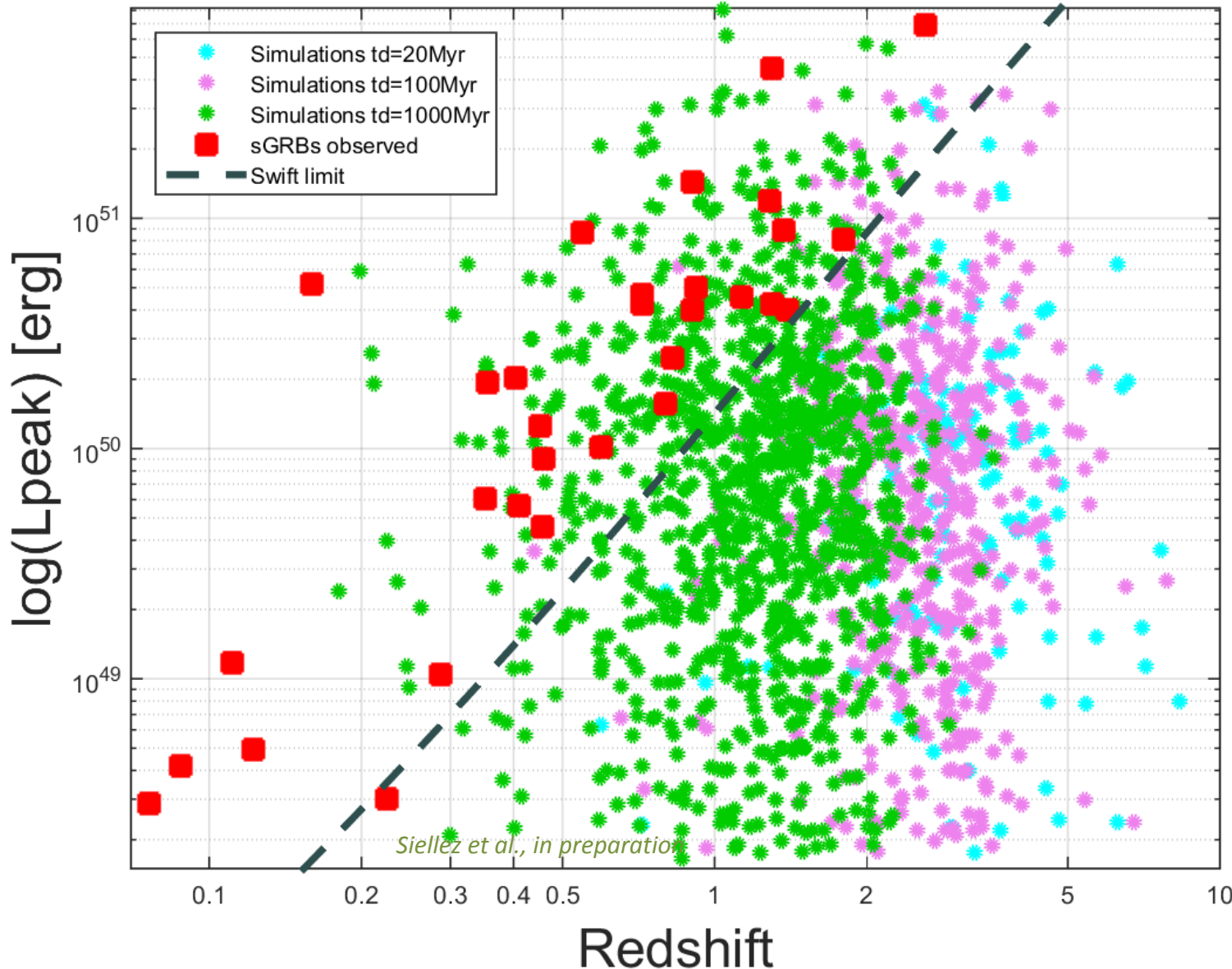
Lpeak (z) : Different delays



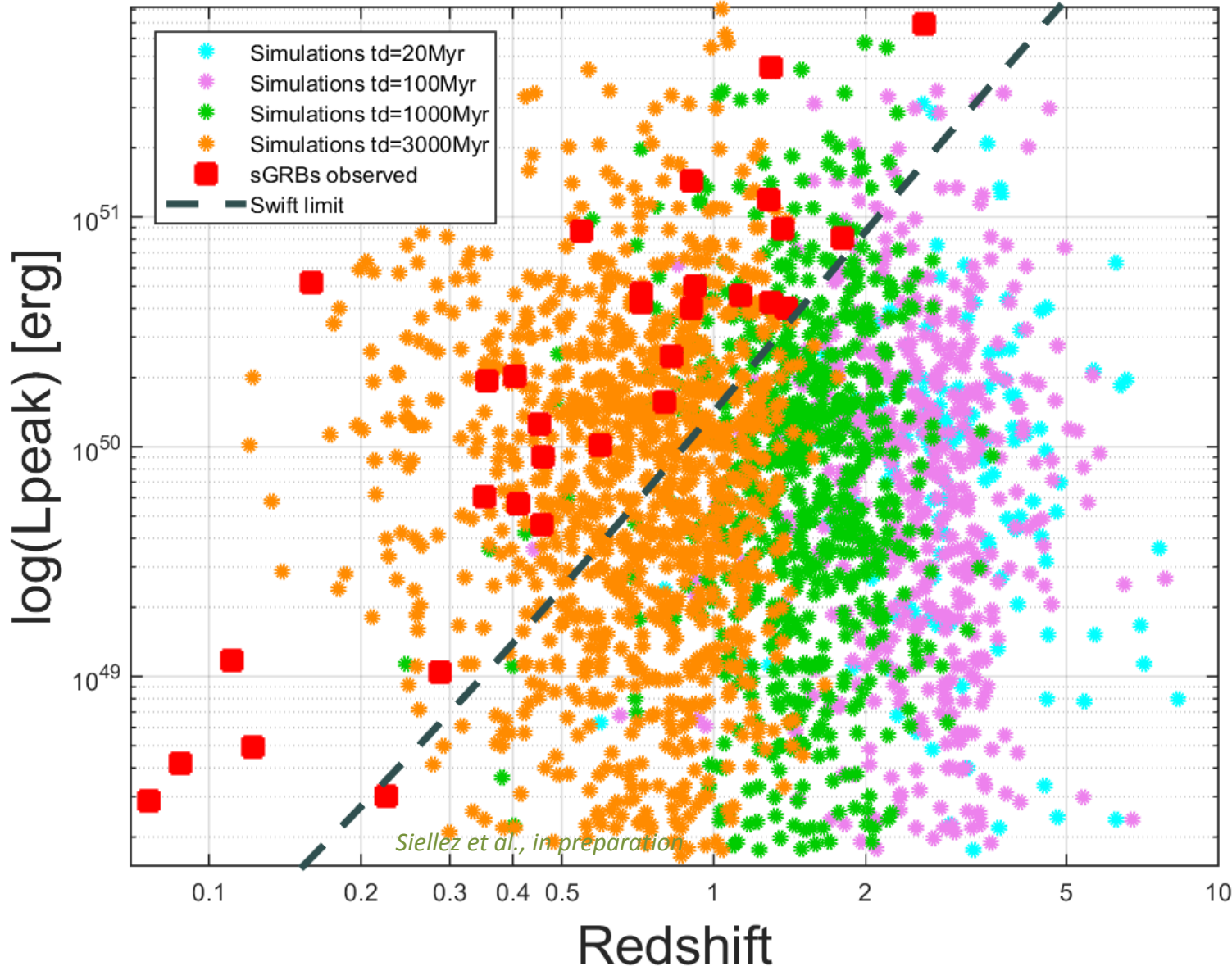
Lpeak (z) : Different delays



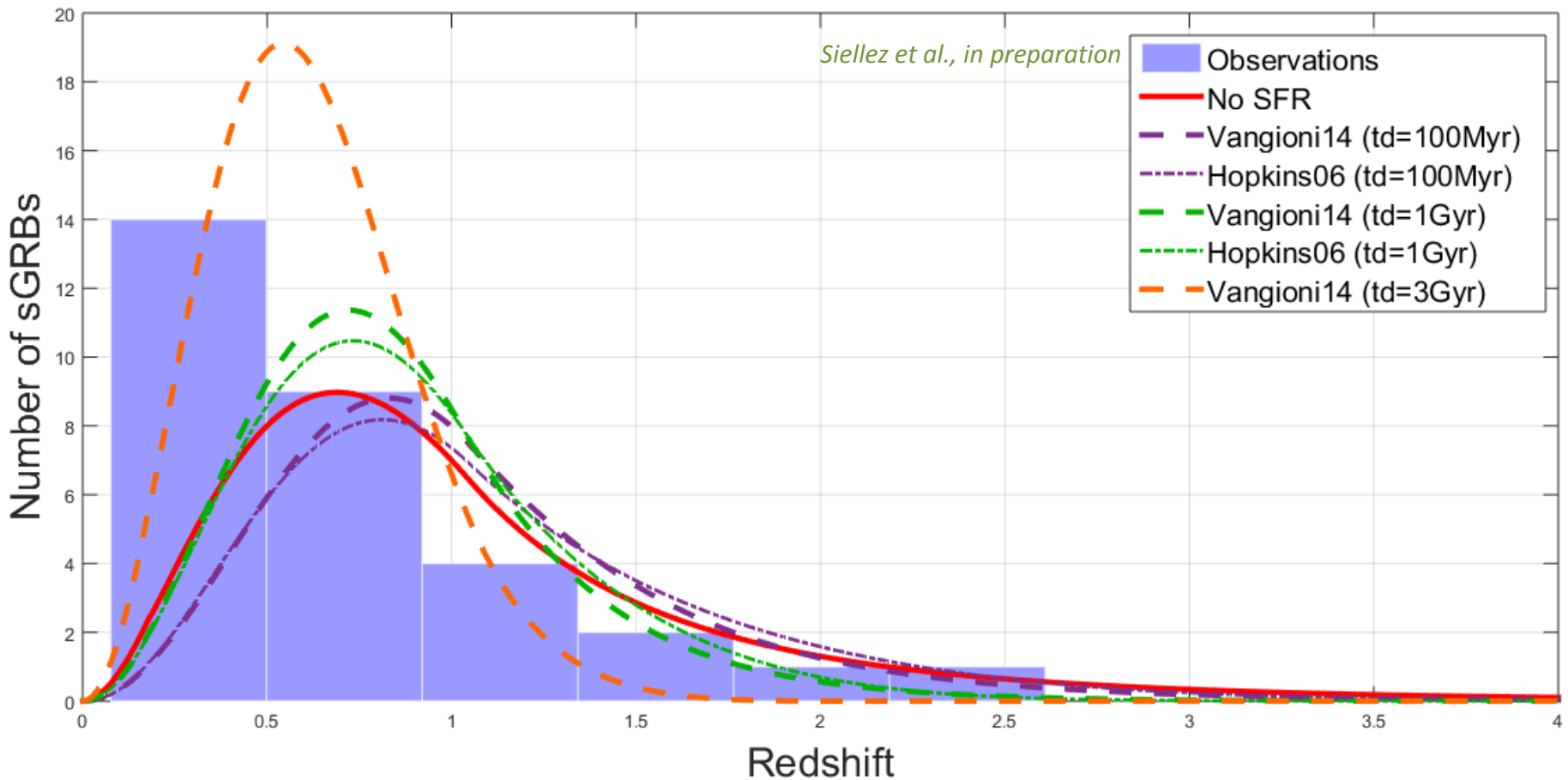
Lpeak (z) :: Different delays



Lpeak (z) : Different delays



Lpeak (z) : Distribution



Summary

- Simulations of the sGRBs observed, using the standard luminosity peak and redshift distribution
=> **impossible to reproduce the low-z low- L_{peak} sGRBs**
- New populations
=> **2 populations of CBC ? Producing sGRBs**
- More statistic ? Guiriec et al. 2015 (ArXiV:1501.07028)
- Influence on the coincident detection rate (Siellez et al. 2014, MNRAS,437,649)

Thank you ... questions and comments are welcoming

That's all Folks!

CBC

GW

Sample of Zhang et al., 2012, ApJ, 755:55

Table 1
A Sample ($N = 17$) of Short GRBs with Measured Redshifts

GRB ^a	T_{90} (s)	z	P^b (10^{-6} erg cm $^{-2}$ s $^{-1}$)	Range (keV)	L_p (10^{51} erg s $^{-1}$)	K^c	$E_{p,i}^b$ (keV)	Refs
050509B	0.04	0.225	0.51 ± 0.3	15–350	0.009 ± 0.004	2.8	$102 \pm [10]$	(6,6,5,5)
050709	0.07	0.16	5.1 ± 0.5	2–400	0.53 ± 0.05	1.5	100 ± 19	(7,2,2,7)
050813	0.6	1.8	0.41 ± 0.19	15–350	16.07 ± 7.5	1.7	$150 \pm [15]$	(6,6,5,5)
051221A	1.4	0.547	46 ± 13	20–2000	69.1 ± 6	1.2	621 ± 144	(6,6,5,5)
060502B	0.131	0.287	1.89 ± 1.49	15–350	0.04 ± 0.01	2.7	$193 \pm [19]$	(6,6,5,5)
061006 ^d	1	0.4377	21 ± 2	20–2000	17.8 ± 2.3	1	955 ± 267	(1,2,2,2)
061201	0.76	0.111	2.45 ± 1.95	15–350	1.27 ± 0.25	1.3	969 ± 508	(6,6,5,5)
061217	0.21	0.827	0.44 ± 0.2	15–350	2.49 ± 1.1	1.7	$216 \pm [22]$	(6,6,5,5)
070429B	0.47	0.904	0.43 ± 0.14	15–350	3.37 ± 1.08	1.9	$813 \pm [81]$	(6,6,5,5)
070714B ^d	2	0.92	1.2 ± 0.9	15–350	14 ± 1	1	2150 ± 1113	(3,2,2,2)
070724A	0.4	0.457	0.14 ± 0.06	15–350	0.23 ± 0.11	2.2	119 ± 12	(6,6,5,5)
070809	1.3	0.2187	0.17 ± 0.08	15–350	0.05 ± 0.02	1.9	$91 \pm [9]$	(6,6,5,5)
071020 ^e	4	2.145	6 ± 0.6	20–2000	220 ± 10	1	1013 ± 205	(4,2,2,2)
071227 ^d	1.8	0.383	3.5 ± 1.1	20–1300	3.11 ± 1.28	1.8	$1383 \pm [138]$	(6,6,5,5)
080913A ^e	8	6.7	0.13 ± 0.08	15–350	114 ± 15	1	1009 ± 200	(4,2,2,2)
090426	1.2	2.609	0.34 ± 0.23	15–350	18.22 ± 5.7	2.1	177 ± 82	(6,6,5,5)
090510 ^d	0.3	0.903	$40 \pm [4]$	8–40000	516 ± 112	0.6	8373 ± 761	(6,6,8,8)

Notes. References are given in order of duration, redshift, peak flux, and rest-frame peak energy, respectively. (1) Hurley et al. 2006, GCN 5702; (2) Ghirlanda et al. 2009; (3) Kodaka et al. 2007, GCN 6637; (4) Greiner et al. 2009; (5) Butler et al. 2007 (<http://butler.lab.asu.edu/swift/>); (6) <http://heasarc.nasa.gov/docs/swift/swiftsc.html>; (7) Villasenor et al. 2005; (8) Ackermann et al. 2010.

^a GRBs 051221A, 061201, and 071227 are discovered by the Konus wind; GRBs 090510 and 050709 are detected by *Fermi*/GBM and HETE-2, respectively; the other 12 bursts are observed by *Swift*/BAT.

^b Values without measured errors have been given a 10% fluctuation, as shown by square brackets.

^c The value of $K = 1$ has been assigned to the four GRBs selected from Ghirlanda et al. (2009).

^d “Short” GRBs with extended emission. GRB 090510 is taken from Abdo et al. (2009), others are drawn from Norris et al. (2010).

^e “Long” GRBs with short-hard properties (see the text in Section 2).

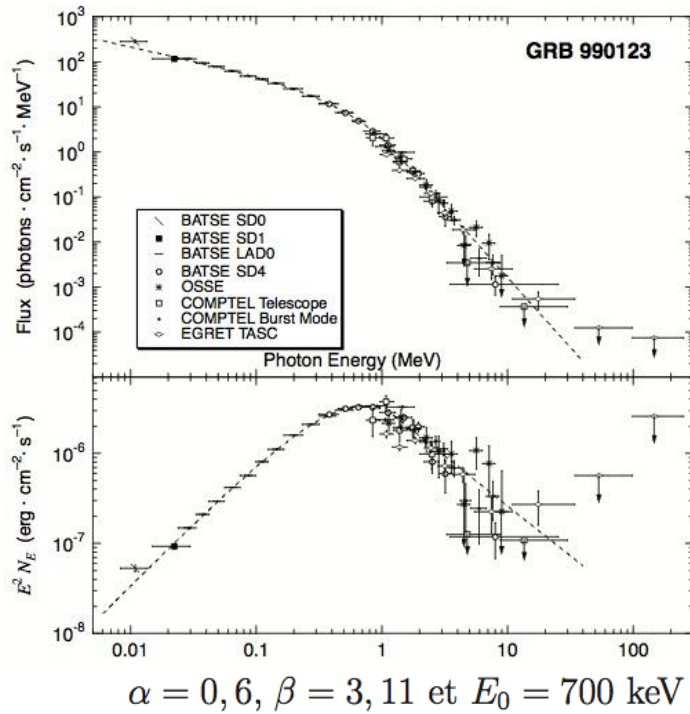
Sample of Zhang et al., 2012, ApJ, 755:55

GRB	Durée [s]			Redshift	Détermination	Références	BAT	Instruments	
	Observée	Intrinsèque	Indice photonique [15-150 keV]					GBM	KONUS
150423A	0.22	0.09	0.84, PL (0.24)	1.394	A	S	X		
150120A	1.20	0.82	1.81, PL (0.18)	0.460	E	S	X	X	
141212A	0.30	0.19	1.61, PL (0.23)	0.596	Host	S	X		
140903A	0.30	0.22	1.99, PL (0.12)	0.351	A	S	X		
131004A	1.54	0.90	1.81, PL (0.11)	0.71	E	S	X	X	
130603B	0.18	0.13	0.82, PL (0.07)	0.356	A + E	S	X		
120804A	0.80	0.35	1.34, PL (0.08)	1.3	Host	1	X		
111117A	0.47	0.20	0.65, PL (0.22)	1.31 ^{+0.46} _{-0.23}	Host	2,3	X	X	X
101219A	0.60	0.35	0.63, PL (0.09)	0.718	Host	S	X		
100724A	1.40	0.61	1.92, PL (0.21)	1.288	A	S	X		
100625A	0.33	0.23	0.90, PL (0.10)	0.452 ± 0.002	Host	4	X	X	X
100206A	0.12	0.08	0.63, PL (0.17)	0.41	Host	S	X	X	
100117A	0.30	0.16	0.88, PL (0.22)	0.915	Host	5	X	X	
090927	2.20	0.93	1.80, PL (0.20)	1.37	A	S	X	X	
090515	0.036	0.026	0.05, CPL (1.36)	0.403	Host	6	X		
090510	0.30	0.16	0.98, PL (0.20)	0.903	E	S	X	X	
090426	1.20	0.33	1.93, PL (0.22)	2.609	A	S	X		
090417A	0.072	0.066	0.65, CPL (2.11)	0.088	Host	7	X		
080905A	1.00	0.89	0.85, PL (0.24)	0.1218	Host	8	X		
070923	0.05	0.046	1.02, PL (0.29)	0.076	Host	9	X		
070729	0.90	0.50	0.27 (n/a)	0.8 ± 0.1	Host	10	X		
070724A	0.40	0.27	1.81, PL (0.33)	0.457	Host	S	X		
070429B	0.47	0.25	1.72, PL (0.23)	0.904	Host	S	X		
061217	0.21	0.11	0.86, PL (0.30)	0.827	E	S	X		
061201	0.76	0.68	0.81, PL (0.15)	0.111	Host	S	X		
060801	0.49	0.23	0.47, PL (0.24)	1.1304	Host	11	X		
060502B	0.13	0.10	0.98, PL (0.19)	0.287	A	S	X		
051221A	1.40	0.90	1.39, PL (0.06)	0.547	E	S	X		
050813	0.45	0.16	1.28, PL (0.37)	1.8	Host	S	X		
050709	0.07	0.06		0.16	Host	12		HETE2	
050509B	0.073	0.060	1.57, PL (0.38)	0.225	A	S	X		

Table of the sample of sGRBs with their observed duration T_{90} and intrinsic duration τ_{90} , their spectral parametra calculated thanks to their distance (redshift z). Références pour z : S sont les données issues de la table Swift : http://swift.gsfc.nasa.gov/archive/grb_table.html/ ; [1] : Berger et al. (2013), [2] : Sakamoto et al. (2013), [3] : Margutti et al. (2012), [4] : Fong et al. (2013), [5] : Fong et al. (2011), [6] : Berger (2010), [7] : O'Brien & Tanvir (2009), [8] : Rowlinson et al. (2010), [9] : Fox & Ofek (2007), [10] : Leibler & Berger (2010), [11] : Berger (2009), [12] : Fox et al. (2005)..

Selection of short GRB

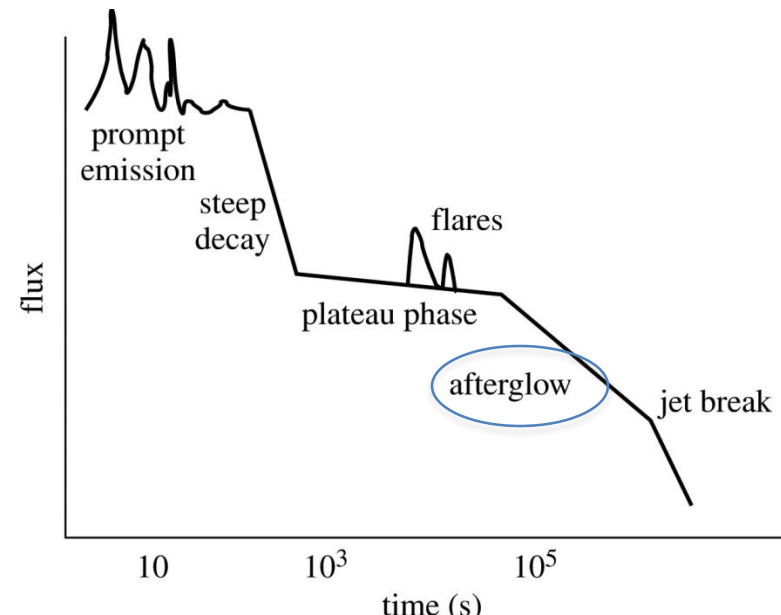
Spectral properties : Band model



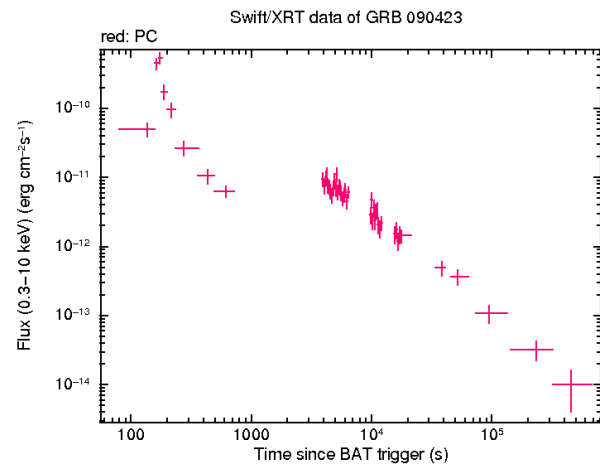
Low Energy :
harder
 $N(E) \propto E^{-\alpha}$
 $0,6 \lesssim \alpha \lesssim 1,5$

High Energy :
softer
 $N(E) \propto E^{-\beta}$
 $2 \lesssim \beta \lesssim 4$

Curve of light

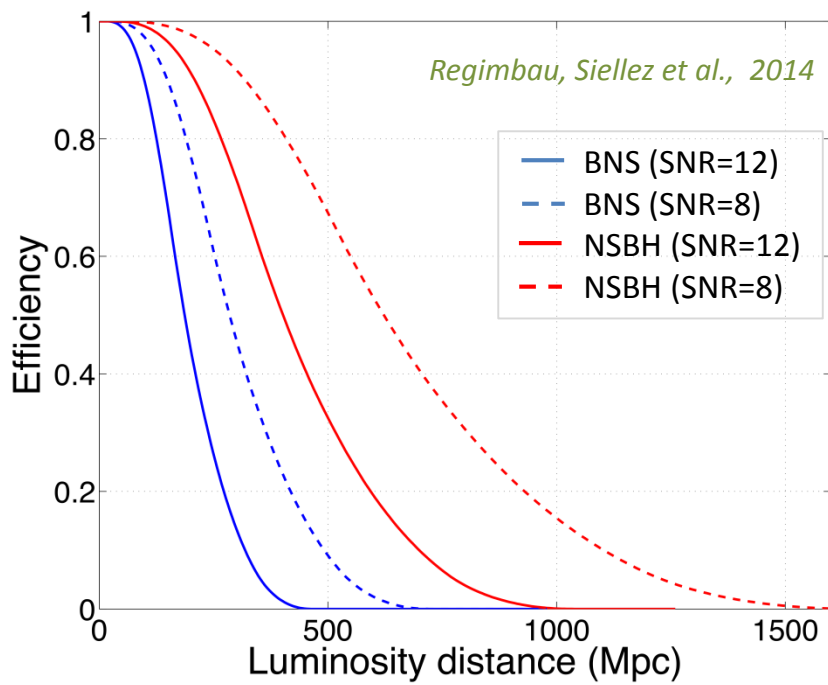


Example

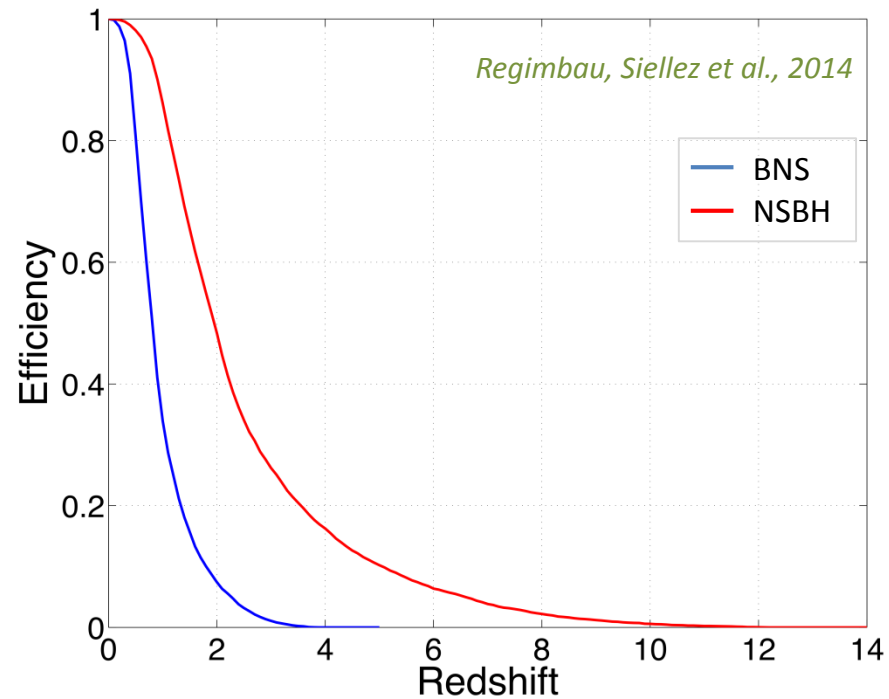


Gravitational wave efficiency

ALV



ET



Efficiency for BNS – Perfect detector

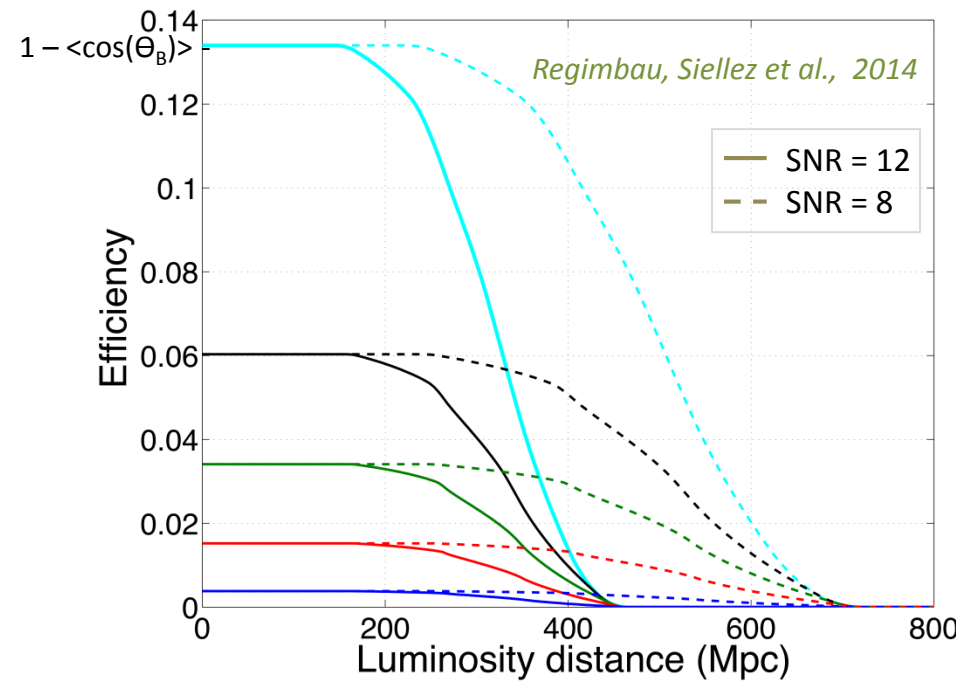
Perfect detector:

DC = 100% ; **FOV** = 4π sr ;

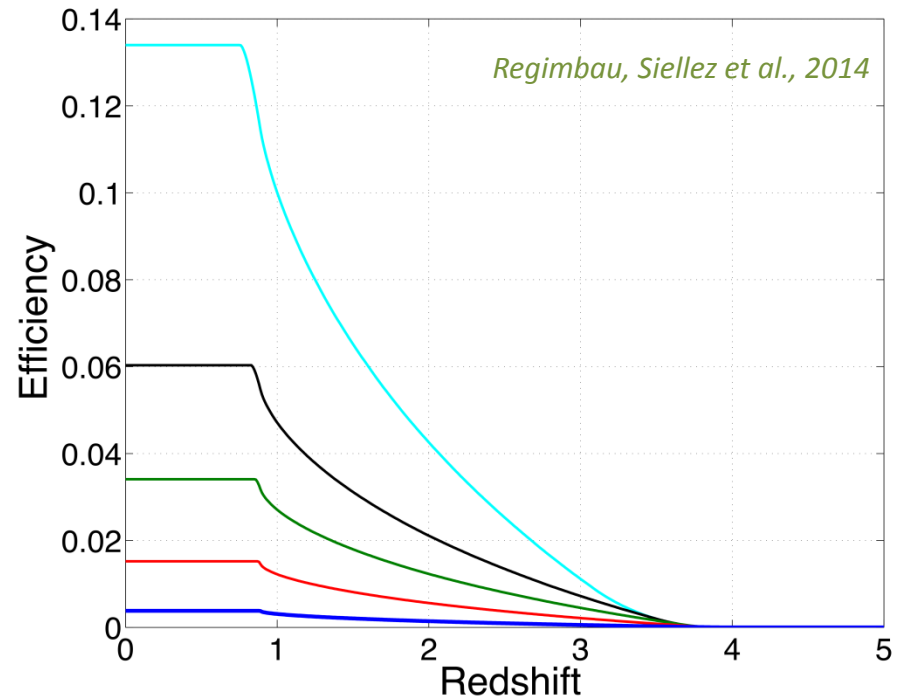
Sensitivity: Infinite

- $\dot{\rho}_c^o \sim 0.06 \text{ Mpc}^{-3} \text{Myr}^{-1}$
- $\Theta_B = 30^\circ, \Theta_B = 20^\circ,$
 $\Theta_B = 15^\circ, \Theta_B = 10^\circ, \Theta_B = 5^\circ.$

ALV



ET



Efficiency for BNS – Realistic detector

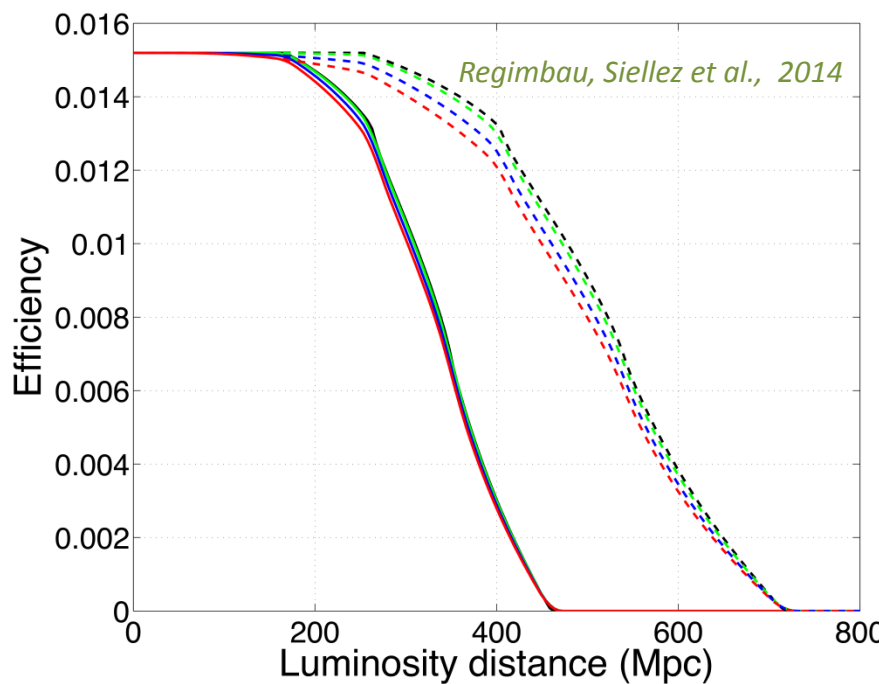
Realistic detector:

DC = 80% ; FOV = 1.4 sr ;

Sensitivity: Infinite, $F_{\text{lim}} = 0.56 \text{ ph s}^{-1} \text{ cm}^{-2}$,
 $F_{\text{lim}} = 1.5 \text{ ph s}^{-1} \text{ cm}^{-2}$, $F_{\text{lim}} = 2.5 \text{ ph s}^{-1} \text{ cm}^{-2}$.

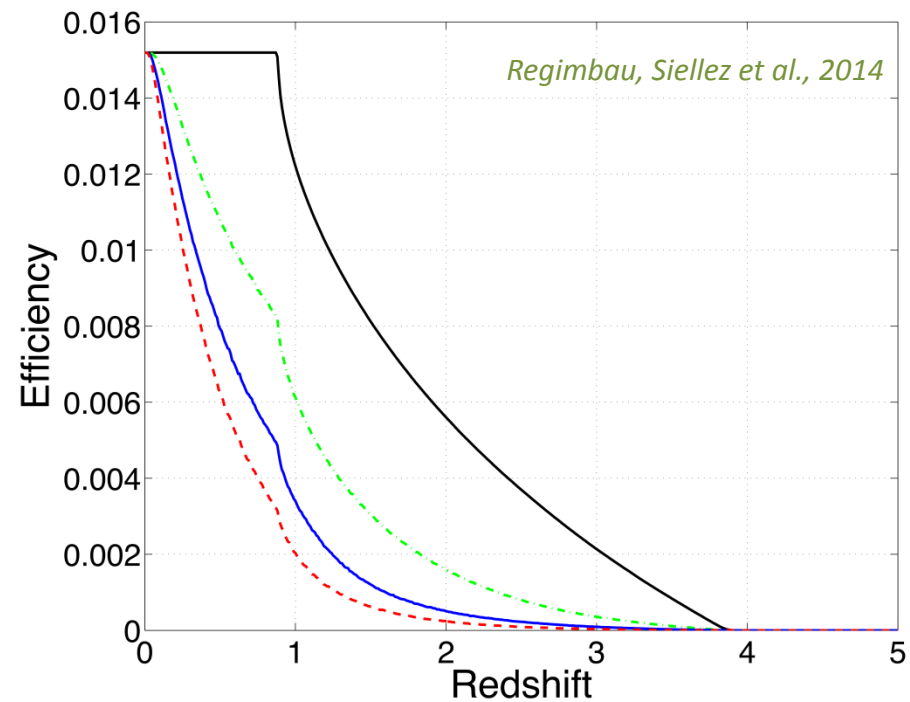
- $\dot{\rho}_c^o \sim 0.06 \text{ Mpc}^{-3} \text{ Myr}^{-1}$
- $\Theta_B = 10^\circ$

ALV



Limited by the GW detectors

ET



Limited by the flux threshold of the GRB detector

Constraints on the beaming angle

Non biased estimator factor : $\hat{\Theta}_B = (\varepsilon_{FOV} \times \varepsilon_{DC}) \frac{N_{cd}^0}{N_{GW}^0}$

